Published in final edited form as:
J Mol Biol. 2003 September 5; 332(1): 23–30.

Nucleotide Binding Induces Changes in the Oligomeric State and Conformation of Sec A in a Lipid Environment: A Small-angle Neutron-scattering Study

Zimei Bu, **Ligong Wang**, and **Debra A. Kendall***
Department of Molecular and Cell Biology, University of Connecticut, 91 N. Eagleville Road Storrs, CT 06269-3125, USA

Abstract

In *Escherichia coli*, SecA is a large, multifunctional protein that is a vital component of the general protein secretion pathway. In its membrane-bound form it functions as the motor component of the protein translocase, perhaps through successive rounds of membrane insertion and ATP hydrolysis. To understand both the energy conversion process and translocase assembly, we have used contrast-matched, small-angle neutron-scattering (SANS) experiments to examine SecA in small unilamellar vesicles of *E. coli* phospholipids. In the absence of nucleotide, we observe a dimeric form of SecA with a radius of gyration comparable to that previously observed for SecA in solution. In contrast, the presence of either ADP or a non-hydrolyzable ATP analog induces conversion to a monomeric form. The larger radius of gyration for the ATP-bound relative to the ADP-bound form suggests the former has a more expanded global conformation. This is the first direct structural determination of SecA in a lipid bilayer. The SANS data indicate that nucleotide turnover can function as a switch of conformation of SecA in the membrane in a manner consistent with its proposed role in successive cycles of deep membrane penetration and release with concommitant preprotein insertion.

Keywords

SecA; oligomerization; nucleotide; protein transport; small-angle neutron scattering

Many proteins that are synthesized in the cytoplasm of cells use the Sec translocase for routing to non-cytoplasmic locations. In *Escherichia coli*, SecYEG and SecA are critical components of this translocase that function in concert with the preprotein to ensure its passage through the membrane. SecYEG can be isolated and purified as a stable heterotrimeric complex,[1-5] and constitutes the central component of the membrane-embedded translocase. SecA is a large, multifunctional protein that is found in both cytoplasmic and membrane-associated forms,[6] and interfaces with SecYEG and the preprotein to propel preprotein translocation at the expense of ATP. Biochemical studies suggest that upon binding ATP[7] and lipid,[8] SecA undergoes a substantial conformational change[9] and is deeply inserted into the membrane bilayer. This membrane association results in stimulation of SecA ATPase activity and preprotein translocation.[10-12]

*Corresponding author: kendall@uconnvm.uconn.edu .
Present address: Z. Bu, Fox Chase Cancer Center, Philadelphia, PA 19111, USA.

A fundamental issue to be resolved is how SecA translates the chemical energy of ATP hydrolysis into the mechanical energy required for preprotein movement. To understand the mechanistic basis for this activity, the structural changes of membrane-associated SecA during nucleotide turnover must be elucidated. This is a complex problem to study, however, because the requirement for the membrane-bound form renders many classical methods of structural analysis of proteins in aqueous solution unfeasible. The SecA-nucleotide cycling event is a dynamic process, making studies in model systems useful for evaluating the species at different stages of nucleotide turnover, yet any such system needs to be physiologically relevant in terms of the content and concentration of components.

Several studies of SecA in aqueous solution indicate that a dimeric form predominates in the presence and in the absence of nucleotide,[13-16] though conditions of lower temperature and higher ionic strength favor a shift toward monomer.[17] The recently reported X-ray structures of *Bacillus subtilis* SecA at 2.7 Å resolution[18] and *Micrococcus tuberculosis* SecA at 2.8 Å resolution[19] also suggests that in aqueous media it forms a dimer that does not undergo a substantial conformational change upon nucleotide binding, consistent with small angle X-ray scattering (SAXS) analysis of SecA, also in an aqueous environment.[14] However, earlier studies involving protease sensitivity, differential scanning calorimetry and dynamic light-scattering suggested that SecA in solution adopts different conformations, depending on the nature of nucleotide bound.[9,20] Measurement of the molar ratio of bound ADP to SecA in solution indicates that only one high-affinity nucleotide-binding site exists per SecA dimer.[21] This and a study involving heterodimers that include ATPase inactive subunits[15] suggest that SecA maintains its dimeric form during translocation, yet recent analysis suggests that the association of SecA with negatively charged phospholipids[22] or detergents[23] shifts the equilibrium toward the monomeric form. The complicated nature of the analyses is illustrated by evidence that the oligomeric state of the SecYE components of the translocase involves a monomer,[24] dimer,[25] and higher-order structure.[26]

Here, we report for the first time the direct structural measurement of the size and shape of SecA in vesicles composed of *E. coli* phospholipids to model the biological membrane. To distinguish SecA features from those of the vesicle, our strategy employed contrast-matched, small-angle, neutron-scattering (SANS) to evaluate SecA in the absence and in the presence of nucleotide. We find that SecA without nucleotide exists in a predominantly dimeric form in this lipid environment that is converted almost exclusively to monomer by the presence of nucleotide. Significant shape differences are observed in the presence of ADP-Mg^{2+} or non-hydrolyzable ATP-Mg^{2+} analog.

Nucleotide binding disrupts SecA dimer in lipid vesicles

We have used SANS to make direct measurements of the structure of SecA in vesicles composed of *E. coli* phospholipids. In addition to providing a model of the physiological membrane, the importance of this lipid composition in promoting ATPase activity[27] and translocation[28] *in vitro* has been demonstrated. Furthermore, the dependence of the signal peptide-stimulated SecA/lipid ATPase activity on a high lipid to protein ratio has been documented[27] and is maintained in the studies here.

The contrast variation experiments require different volume fractions of ^2H_2O to determine the lipid contrast match point at which the scattering intensity from the small unilamellar vesicles (SUV) is zero. As shown in Figure 1(a), this occurs at 14.3% (v/v) ^2H_2O volume fraction. Flotation analysis shows that SecA is lipid-associated (Figure 1(b)). Figure 2(a) shows the Guinier plot of 2.9 mg/ml of SecA and 23 mg/ml of *E. coli* SUV in a 14.3% (v/v) ^2H_2O buffer solution. For the SecA dimer, the Guinier analysis was conducted in the region of $Q \leq 0.027$ Å^{-1} corresponding to $QR_g \leq 1.2$. For the ATP-Mg^{2+} analog and ADP-

Mg^{2+}-bound forms of SecA, the Guinier analysis was conducted in the region of $Q \leq 0.030$ $Å^{-1}$ and $Q \leq 0.034$ $Å^{-1}$, corresponding to $QR_g \leq 1.18$ and $QR_g \leq 1.08$, respectively.

The molecular mass standard bovine serum albumin (BSA 68 kDa) was dissolved with 23 mg/ml of lipid vesicles in 14.3% ^2H_2O (v/v) buffers. The protein concentration-normalized forward scattering intensity ($I(0)/c_{protein}$) was used to calibrate the molecular mass of the different forms of SecA. A calibration of $I(0)c_{protein}$ of SecA against that of BSA gives a molecular mass of 204 kDa for SecA, indicating that it is a dimer at the concentration measured by SANS (see Table 1).

The radius of gyration of SecA in the lipid vesicles determined by SANS is 45.1(±0.9) Å (Table 1), consistent with the previously reported value of 45.2 Å for SecA determined by SAXS in aqueous solution.[14] This indicates that the radius of gyration of the SecA dimer observed by these methods does not change in the presence of *E. coli* lipid vesicles. Flotation analysis confirms that under these conditions SecA is nonetheless associated stably with the vesicles (and Figure 1(b)).[10]

The distance distribution function ($P(r)$) of apo SecA shows that SecA in the presence of lipid vesicles is a dimer, whereas the dimer dissociates upon binding ATP or ADP (Figure 2(b)). The asymmetric shape of $P(r)$ suggests the SecA dimer is asymmetric. Our SANS results for the SecA dimer without nucleotide in lipid vesicles are thus in approximate agreement with the SAXS study of SecA in solution,[14] although the shape of the SecA dimer seems to be more expanded in lipid relative to that in aqueous buffer (160 Å *versus* 150 Å).

Figure 2(a) shows the Guinier plot of SecA at 2.9 mg/ml of SUV in the presence of non-hydrolyzable ATP analog and Mg^{2+} . The protein concentration-normalized forward scattering intensity is about half of that of the apo SecA, shown in Figure 2(a), indicating that the molecular mass of the ATP analog-bound form of SecA is half of the apo SecA in lipid. The molecular mass calculated from $I(0)/c_{protein}$ against a molecular mass standard, BSA, shows that the ATP analog-bound form of SecA is a monomer at the concentration measured by SANS (Table 1). Similarly, the $I(0)/c_{protein}$ of SecA in the presence of ADP and Mg^{2+} is about half of that of SecA, indicating that the ADP-bound form of SecA is a monomer. In contrast, SAXS indicated that SecA in aqueous solution remained dimeric even in the presence of nucleotide.[14]

The ATP-bound SecA monomer is more expanded than the ADP-bound SecA monomer

Based on a K_d of 0.8 μM ADP for SecA in solution,[21] and an estimate of the K_d for the non-hydolyzable ATP analog,[29] we have studied SecA in the presence of nucleotide sufficient to yield >97% occupancy of the high-affinity nucleotide-binding site on SecA. From the Guinier plots (Figure 2(a)), the radius of gyration of SecA–ATP-Mg^{2+} is R_g = 38.3(±0.8) Å, larger than the radius of gyration of SecA–ADP-Mg^{2+} of R_g = 31.1(±0.5) Å. This suggests that the ATP-bound form of the monomeric SecA has a more expanded global conformation than the ADP-bound, monomeric form. The $P(r)$ of the ATP-bound and the ADP-bound forms of SecA show that the SecA dimer dissociates upon binding ATP or ADP (Figure 2(b)), and the maximum dimension of the SecA–ATP-Mg^{2+} form is larger than that of the SecA–ADP-Mg^{2+} form (about 125 Å and 105 Å, respectively).

The K_d for the monomer-dimer equilibrium of SecA in aqueous solution in the absence of nucleotide is estimated to be in the submicromolar to low micromolar range.[13,17] The corresponding values in the presence of lipid vesicles and/or nucleotides remain undefined.

A recent study of SecA using fluorescence resonance energy transfer suggests that in the presence of membranes containing acidic phospholipids, SecA dissociates into monomers.[22] The concentration of SecA used in the fluorescence resonance energy transfer experiment was about 1.5 μM, while the concentration used in the SANS experiment was about 28 μM, suggesting that these experiments were run just below and above, respectively, the K_d for dimer dissociation in the absence of nucleotide. Collectively, the data suggest that the presence of the lipid environment shifts the K_d upward into the micromolar range and the presence of nucleotide increases the K_d value even further, resulting in a species that is predominantly monomeric. The physiological concentration of SecA is estimated at about 10 μM for the bulk volume of the bacterium[16,22] yet is effectively higher at the translocon due to the concentrating effect of binding to specific sites comprised of SecYEG. Therefore, our SANS experiments likely provide a good physiological representation of the local concentration in this environment. Furthermore, our observation that SecA forms a dimer in the absence of nucleotide is consistent with the finding that the dimeric species can associate with the biological membrane *in vitro*.[15] However, since those experiments involved ongoing protein translocation and continual nucleotide turnover, individual SecA states formed during that process could not be distinguished. An advantage of the strategy we have employed here is the ability to distinguish distinct structural states under defined conditions. Moreover, we have been able to characterize the dimensions of SecA in the presence of a bilayer composed of *E. coli* phospholipids. In this environment, nucleotide modulates substantial SecA conformation changes, consistent with previous biochemical analyses in membranes.[30-32] This underscores the role of the ATPase activity in the membrane interactive species and the possibility that the accompanying changes in conformation serve to propel the preprotein through the translocon.

The maximum dimension (D_{max}) of the SecA–ATP-Mg^{2+} form is about 125 Å and the D_{max} of SecA–ADP-Mg^{2+} form is about 105 Å (Figure 2(b)). We have used the program DAMMIN[33] to calculate the envelopes of the different forms of SecA. Figure 3(a) is the calculated envelope based on the crystal structure of *B. subtilis* SecA in an aqueous environment[18] published while we were preparing this manuscript, and Figure 3(b) and (c) are envelopes of the ATP analog-bound and ADP-bound forms, respectively, of SecA calculated from SANS data. The envelopes shown in Figure 3 provide a direct view of the structural changes of SecA upon binding to nucleotides.

The crystal structure[18,19] of SecA can be considered to contain three domains: the preprotein-binding domain, the first nucleotide-binding fold (NBFI), and the second nucleotide-binding fold (NBFII). The actual nucleotide-binding site is in the cleft between NBFI and NBFII. In this spirit, the structure of SecA resembles the structure of a single subunit of GroEL which is composed of three domains: the apical domain that binds to unfolded protein, the intermediate domain and the equatorial domain. The nucleotide-binding site on GroEL is in the cleft formed between the intermediate and the equatorial domains.[34,35] When bound to ATP, the intermediate domain of GroEL orients in such a way as to push the apical domain further from the equatorial domain through rigid body movement.[34-39] In the ADP-bound form, the intermediate domain reorients itself to bring the apical domain and the equatorial domain closer into a more compact form. Based on our analysis of the structural analogy of SecA with a single subunit of GroEL, we hypothesize that nucleotide-binding induces similar conformation changes in both proteins and these two proteins may share common features in the reaction cycles of nucleotide binding and hydrolysis, and interacting with the unfolded proteins. In the case of SecA, these conformational changes are consistent with models for processive chain movement;[40,41] the more expanded ATP-bound form is well suited for traversing the membrane carrying a portion of the preprotein, while subsequent hydrolysis triggers the release of the preprotein, generation of the more compact form of SecA and its retraction to the cytoplasmic face of

the membrane. ADP-ATP exchange could then serve to initiate another cycle of structural changes with insertion and de-insertion to processively transport successive segments of the preprotein. Further, that nucleotide does not induce these conformational changes in the absence of membranes serves to dedicate its function in preprotein processivity to the locale of the translocon and inhibit the likelihood that SecA in the cytoplasm participates non-productively in this activity.

Acknowledgments

We thank Sharyn Rusch for helpful discussions and critically reading this manuscript. This research was supported, in part, by National Institutes of Health grant GM37639 (to D.A.K.). This work utilized facilities supported, in part, by the National Science Foundation under agreement no. DMR-9986442.

Abbreviations used

AMP-PNP	5′-adenylylimidodiphosphate
BSA	bovine serum albumin
SUV	small unilamellar vesicles
SANS	small-angle neutron-scattering
SAXS	small angle X-ray scattering
SUV	small unilamellar vesicles

References

1. Brundage L, Hendrick JP, Schiebel E, Driessen AJ, Wickner W. The purified *E. coli* integral membrane protein SecY/E is sufficient for reconstitution of SecA-dependent precursor protein translocation. Cell. 1990; 62:649–657. [PubMed: 2167176]
2. Brundage L, Fimmel CJ, Mizushima S, Wickner W. SecY, SecE, and band 1 form the membrane-embedded domain of *Escherichia coli* preprotein translocase. J. Biol. Chem. 1992; 267:4166–4170. [PubMed: 1531482]
3. Douville K, Price A, Eichler J, Economou A, Wickner W. SecYEG and SecA are the stoichiometric components of preprotein translocase. J. Biol. Chem. 1995; 270:20106–20111. [PubMed: 7650029]
4. Hanada M, Nishiyama KI, Mizushima S, Tokuda H. Reconstitution of an efficient protein translocation machinery comprising SecA and the three membrane proteins, SecY, SecE, and SecG (p12). J. Biol. Chem. 1994; 269:23625–23631. [PubMed: 8089132]
5. Akimaru J, Matsuyama S, Tokuda H, Mizushima S. Reconstitution of a protein translocation system containing purified SecY, SecE, and SecA from *Escherichia coli*. Proc. Natl Acad. Sci. USA. 1991; 88:6545–6549. [PubMed: 1830665]
6. Cabelli RJ, Dolan KM, Qian LP, Oliver DB. Characterization of membrane-associated and soluble states of SecA protein from wild-type and SecA51(TS) mutant strains of *Escherichia coli*. J. Biol. Chem. 1991; 266:24420–24427. [PubMed: 1837021]
7. Mitchell C, Oliver D. Two distinct ATP-binding domains are needed to promote protein export by *Escherichia coli* SecA ATPase. Mol. Microbiol. 1993; 10:483–497. [PubMed: 7968527]
8. Ulbrandt ND, London E, Oliver DB. Deep penetration of a portion of *Escherichia coli* SecA protein into model membranes is promoted by anionic phospholipids and by partial unfolding. J. Biol. Chem. 1992; 267:15184–15192. [PubMed: 1386084]
9. Shinkai A, Mei LH, Tokuda H, Mizushima S. The conformation of SecA, as revealed by its protease sensitivity, is altered upon interaction with ATP, presecretory proteins, everted membrane vesicles, and phospholipids. J. Biol. Chem. 1991; 266:5827–5833. [PubMed: 1826005]
10. Lill R, Dowhan W, Wickner W. The ATPase activity of SecA is regulated by acidic phospholipids, SecY, and the leader and mature domains of precursor proteins. Cell. 1990; 60:271–280. [PubMed: 2153463]

11. Lill R, Cunningham K, Brundage LA, Ito K, Oliver D, Wickner W. SecA protein hydrolyzes ATP and is an essential component of the protein translocation ATPase of *Escherichia coli*. EMBO J. 1989; 8:961–966. [PubMed: 2542029]
12. Cunningham KW, Wickner WT. Specific recognition of the leader region of precursor proteins is required for the activation of translocation ATPase of *Escherichia coli*. Proc. Natl Acad. Sci. USA. 1989; 86:8630–8634. [PubMed: 2554321]
13. Doyle SM, Braswell EH, Teschke CM. SecA folds *via* a dimeric intermediate. Biochemistry. 2000; 39:11667–11676. [PubMed: 10995234]
14. Shilton B, Svergun DI, Volkov VV, Koch MH, Cusack S, Economou A. *Escherichia coli* SecA shape and dimensions. FEBS Letters. 1998; 436:277–282. [PubMed: 9781695]
15. Dreissen AJM. SecA, the peripheral subunit of the *Escherichia coli* precursor protein translocase, is functional as a dimer. Biochemistry. 1993; 32:13190–13197. [PubMed: 8241173]
16. Akita M, Shinkai A, Matsuyama S, Mizushima S. SecA, an essential component of the secretory machinery of *Escherichia coli*, exists as homodimer. Biochem. Biophys. Res. Commun. 1991; 174:211–216. [PubMed: 1824919]
17. Woodbury RL, Hardy SJ, Randall LL. Complex behavior in solution of homodimeric SecA. Protein Sci. 2002; 11:875–882. [PubMed: 11910030]
18. Hunt JF, Weinkauf S, Henry L, Fak JJ, McNicholas P, Oliver DB, Deisenhofer J. Nucleotide control of interdomain interactions in the conformational reaction cycle of SecA. Science. 2002; 297:2018–2026. [PubMed: 12242434]
19. Sharma V, Arockiasamy A, Ronning DR, Savva CG, Holzenburg A, Braunstein M, et al. Crystal structure of *Mycobacterium tuberculosis* SecA, a preprotein translocating ATPase. Proc. Natl Acad. Sci. USA. 2003; 100:2243–2248. [PubMed: 12606717]
20. den Blaauwen T, Fekkes P, de Wit JG, Kuiper W, Driessen AJM. Domain interactions of the peripheral preprotein translocase subunit SecA. Biochemistry. 1996; 35:11994–12004. [PubMed: 8810904]
21. Schmidt M, Ding H, Ramamurthy V, Mukerji I, Oliver D. Nucleotide binding activity of SecA homodimer is conformationally regulated by temperature and altered by prlD and azi mutations. J. Biol. Chem. 2000; 275:15440–15448. [PubMed: 10747939]
22. Or E, Navon A, Rapoport T. Dissociation of the dimeric SecA ATPase during protein translocation across the bacterial membrane. EMBO J. 2002; 21:4470–4479. [PubMed: 12198149]
23. Benach J, Chou YT, Fak JJ, Itkin A, Nicolae DD, Smith PC, et al. Phospholipid-induced monomerization and signal-peptide-induced oligomerization of SecA. J. Biol. Chem. 2003; 278:3628–3638. [PubMed: 12403785]
24. Yahr TL, Wickner WT. Evaluating the oligomeric state of SecYEG in preprotein translocase. EMBO J. 2000; 19:4393–4401. [PubMed: 10944122]
25. Bessonneau P, Besson V, Collinson I, Duong F. The SecYEG preprotein translocation channel is a conformationally dynamic and dimeric structure. EMBO J. 2002; 21:995–1003. [PubMed: 11867527]
26. Manting EH, van der Does C, Remigy H, Engel A, Driessen AJ. SecYEG assembles into a tetramer to form the active protein translocation channel. EMBO J. 2000; 19:852–861. [PubMed: 10698927]
27. Miller A, Wang L, Kendall DA. Synthetic signal peptides specifically recognize SecA and stimulate ATPase activity in the absence of preprotein. J. Biol. Chem. 1998; 273:11409–11412. [PubMed: 9565549]
28. Henrick JP, Wickner W. SecA protein needs both acidic phospholipids and SecY/E protein for functional high-affinity binding to the *Escherichia coli* plasma membrane. J. Biol. Chem. 1991; 266:24596–24600. [PubMed: 1837025]
29. Matsuyama S, Kimura E, Mizushima S. Complementation of two overlapping fragments of SecA, a protein translocation ATPase of *Escherichia coli*, allows ATP binding to its amino-terminal region. J. Biol. Chem. 1990; 265:8760–8765. [PubMed: 2160468]
30. Ramamurthy V, Oliver D. Topology of the integral membrane form of *Escherichia coli* SecA protein reveals multiple periplasmically exposed regions and modulation by ATP binding. J. Biol. Chem. 1997; 272:23239–23246. [PubMed: 9287332]

31. Eichler J, Wickner W. Both an N-terminal 65-kDa domain and a C-terminal 30-kDa domain of SecA cycle into the membrane at SecYEG during translocation. Proc. Natl Acad. Sci. USA. 1997; 94:5574–5581. [PubMed: 9159114]
32. Ahn T, Kim H. SecA of *Escherichia coli* traverses lipid bilayer of phospholipid vesicles. Biochem. Biophys. Res. Commun. 1994; 203:326–330. [PubMed: 8074674]
33. Svergun DI. Restoring low resolution structure of biological macromolecules from solution scattering using simulated annealing. Biophys. J. 1999; 76:2879–2886. [PubMed: 10354416]
34. Braig K, Otwinowski Z, Hegde R, Boisvert DC, Joachimiak A, Horwich AL, Sigler PB. The crystal structure of the bacterial chaperonin GroEL at 2.8 Å. Nature. 1994; 371:578–586. [PubMed: 7935790]
35. Boisvert DC, Wang J, Otwinowski Z, Horwich AL, Sigler PB. A crystal structure of the bacterial chaperonin GroEL complexed with ATP gamma S. Nature Struct. Biol. 1996; 3:170–177. [PubMed: 8564544]
36. Chen S, Roseman AM, Hunter AS, Wood SP, Burston SG, Ranson NA, et al. Location of a folding protein and shape changes in GroEL–GroES complexes imaged by cryo-electron microscopy. Nature. 1994; 371:261–264. [PubMed: 7915827]
37. Roseman AM, Chen S, White H, Braig K, Saibil HR. The chaperonin ATPase cycle: mechanism of allosteric switching and movements of substrate-binding domains in GroEL. Cell. 1996; 87:241–251. [PubMed: 8861908]
38. Xu Z, Horwich AL, Sigler PB. The crystal structure of the asymmetric GroEL-GroES-(ADP)7 chaperonin complex. Nature. 1997; 388:741–750. [PubMed: 9285585]
39. Ma J, Sigler PB, Xu Z, Karplus M. A dynamic model for the allosteric mechanism of GroEL. J. Mol. Biol. 2000; 302:303–313. [PubMed: 10970735]
40. Economou A, Wickner W. SecA promotes preprotein translocation by undergoing ATP-driven cycles of membrane insertion and deinsertion. Cell. 1994; 78:835–843. [PubMed: 8087850]
41. Economou A, Pogliano JA, Beckwith J, Oliver D, Wickner W. SecA membrane cycling at SecYEG is driven by distinct ATP binding and hydrolysis events and is regulated by SecD and SecF. Cell. 1995; 83:1171–1181. [PubMed: 8548804]
42. Glinka C, Barker J, Hammouda B, Krueger S, Moyer J, Orts W. The 30m SANS instruments at NIST. J. Appl. Crystallog. 1998; 31:430–445.
43. Bu Z, Engelman DM. A method for determining transmembrane helix association and orientation in detergent micelles using small angle X-ray scattering. Biophys. J. 1999; 77:1064–1073. [PubMed: 10423450]
44. Wriggers W, Chacón P. Using situs for the registration of protein structures with low-resolution bead models from X-ray solution scattering. J. Appl. Crystallog. 2001; 34:773–776.

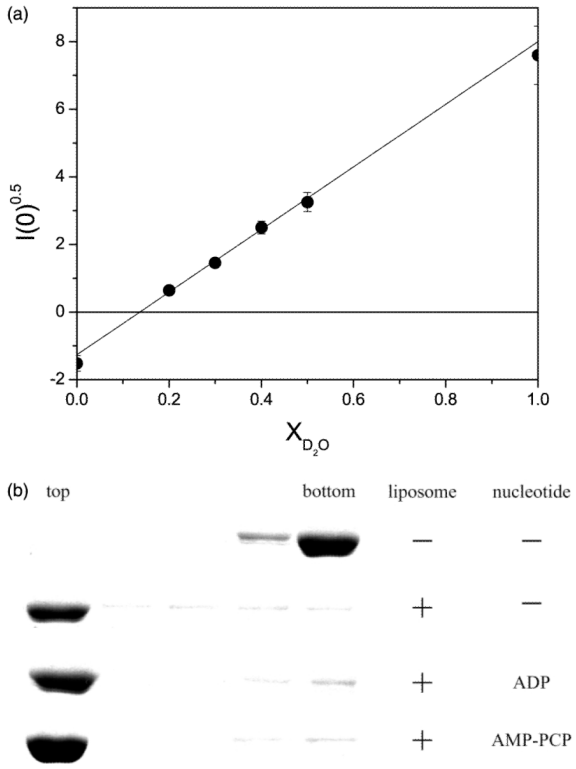

Figure 1.

(a) Contrast variation experiments to determine the match point of *E. coli* SUV. To make SUV, 0.4 ml of 25 mg/ml of chloroform-dissolved *E. coli* polar lipid extract (Avanti Polar Lipids, Inc., AL) was transferred to a 12 ml Pyrex tube. A thin film of lipid was formed under a stream of filtered nitrogen and residual chloroform was removed by high vacuum overnight. The lipid film was then re-hydrated in 1 mM DTT, 50 mM potassium phosphate (pH 7.5), 50 mM KCl, 1 mM EDTA. SUV were formed by sonicating until the solution was optically clear. The contrast variation experiments required different volume fractions of ^2H_2O to determine the lipid contrast match point at which the scattering intensity from the SUV is zero. For contrast variation experiments, the lipid was resuspended separately in H_2O and ^2H_2O buffer to make the two SUV solutions. The H_2O and ^2H_2O SUV solutions were mixed in different proportions to produce six SUV solutions of different ^2H_2O volume fractions. The lipid concentration used for contrast variation experiments was 10 mg/ml. The square-root of scattering intensity $I(0)^{0.5}$, from the SUV as a function of ^2H_2O volume fraction is shown. The contrast match point can be determined from this plot to be $X2_{H_2O}$ = 0.143. At a ^2H_2O volume fraction of 0.143, the scattering intensity from the lipid vesicles is zero, indicating the scattering density contrast between the SUV and the buffer solution is zero. Further experiments on SecA/SUV solutions were therefore conducted at this ^2H_2O concentration to eliminate the scattering from the SUV. (b) Association of SecA with SUV analyzed by flotation gradient centrifugation. SecA (1.5 mg/ml) was mixed with *E. coli* SUV (12 mg/ml) in the aforementioned phosphate buffer with density of 1.29 g/ml adjusted with metrizamide. Magnesium acetate (60 μM) was added when ADP (60 μM) or AMP-PNP (2 mM) was included in buffer. Samples (200 μl) were layered below 400 μl of corresponding buffers with density of 1.27 g/ml. Samples were centrifuged (for 33 hours, at 4°C, at 35,000 rpm) in a Beckman SW50.1 rotor with adapters for 5 × 41 mm Beckman Ultraclear centrifuge tubes, six 100 μl fractions were harvested and the top three and bottom two fractions analyzed by SDS-PAGE and staining with Coomassie brilliant blue.

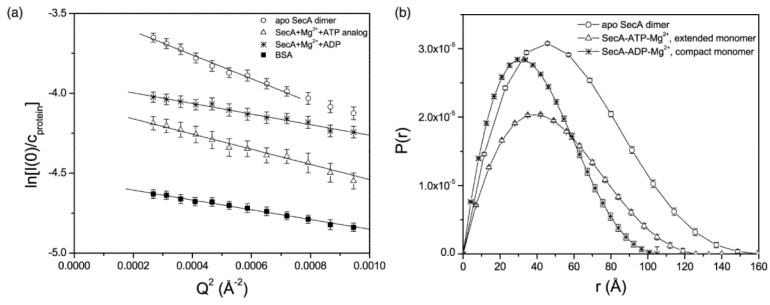

Figure 2.

(a) Guinier plots of SecA, SecA–ATP-Mg^{2+} and SecA–ADP-Mg^{2+} in *E. coli* SUV. *E. coli* SecA was isolated from strain BL21.14 pCS1 as described[7] with greater than 98% purity as assessed by SDS-PAGE, and exhibited characteristic levels of ATPase activity in the presence of lipid.[27] The protein was concentrated to about 20 mg/ml using a 2 ml Centricon with a cut-off of 10 kDa. The protein was then dialyzed against 200 ml of sterilized 50 mM potassium phosphate (pH 7.5), 50 mM KCl, 1 mM EDTA containing 14.3% (v/v) ^2H_2O. This concentration of EDTA was chosen carefully to preclude the possible magnesium-induced liposome aggregation, while ensuring the occupancy of the high-affinity nucleotide-binding site and, under comparable conditions, SecA exhibits ATPase activity. SecA was added to the SUV solution resulting in a concentration of SecA of 2.9 mg/ml and 23 mg/ml of lipid. Under similar conditions, SecA associates stably with vesicles (Figure 1(b)). For the ATP-binding experiment, 2 mM non-hydrolyzable ATP analog (AMP-PNP, 5′-adenylyl imidodiphosphate) and 60 μM Mg^{2+} were added to the SecA/SUV solution. For the ADP-binding experiment, 60 μM ADP and 60 mM Mg^{2+} were added to the SecA/SUV solution. SANS measurements were conducted using the NG-7 30 meter SANS instrument at the National Institute of Standards and Technology (Gaithersburg, MD).[42] The incident neutron wavelength was λ = 6 Å with a wavelength resolution of Δλ/λ = 11%. The sample-to-detector distances were 7 m and 1.5 m to give a *Q* range from 0.006 $Å^{-1}$ to 0.33 $Å^{-1}$. Quartz banjo cells of 1 mm path-length were used. The scattered intensity was placed on an absolute level using a calibrated secondary standard and circularly averaged to yield the scattered intensity, $I(Q)$, as a function of Q. The scattering from the buffer background was measured, corrected by the volume fraction displaced by the protein, and subtracted from the scattering by the protein solution. Data acquisition times were eight hours and 20 minutes at sample-to-detector distances of 7 m and 1.5 m, respectively, for both protein solutions and buffer backgrounds. SANS measurements were performed at room temperature. For a multi-component system, such as a protein/lipid complex, the scattering intensity is:[43]

$$I(Q) = (\rho_p - \rho_s)^2 I'_p(Q) + (\rho_p - \rho_s)(\rho_L - \rho_s) I'_{pL}(Q) + (\rho_L - \rho_s)^2 I'_L(Q) \quad (1)$$

where ρ_L is the averaged scattering density of the lipid vesicles, $I'_L(Q)$ is the scattering from the lipid vesicles, $I'_{pL}(Q)$ is the cross-term reflecting the interference between the scattering amplitudes of the protein and the lipid vesicles. The experiments were conducted at the contrast match point of the lipid so that the scattering intensity from the lipid is zero, and equation (1) is reduced to:

$$I(Q) = (\rho_p - \rho_s)^2 I'(Q) \quad (2)$$

where the scattering intensity, $I(Q)$, is proportional to the square of the contrast $(\rho_p - \rho_s)^2$, where ρ_p is the scattering density of the protein and ρ_s is the scattering density of the buffer. The radius of gyration, R_g, is related to the size and conformation of the protein and can be obtained from the Guinier approximation:

$$\ln \quad I(Q) = \ln \quad I(0) - \frac{1}{3}R_g^2 Q^2 \tag{3}$$

by linear least-squares fitting in the $QR_g \leq 1$ region, where $I(0)$ is the forward scattering intensity that is related to the molecular mass of the macromolecule:

$$I(0) = (\rho_p - \rho_s)^2 c \frac{M_w}{N_A} \bar{v}_p^2 \tag{4}$$

where c is the protein concentration, M_w is the protein molecular mass, N_A is Avogadro's number and $\bar{v}_p$ is the partial specific volume of the protein. Bovine serum albumin (BSA) was used as the molecular mass standard and was dissolved at 11.4 mg/ml in the SUV solution under the conditions used for SecA. The scattering from BSA in the lipid vesicles was used as a control for molecular mass calibration. The scattering intensities of the different forms of SecA and that of BSA were normalized by the protein concentrations. (b) $P(r)$ of SecA, SecA–ATP-Mg^{2+}, SecA–ADP-Mg^{2+}. Inverse Fourier transformation of $I(Q)$ gives the distance distribution function, $P(r)$, which is the probable frequency distribution of the vector length between scattering points in the macromolecules. The D_{max} at which $P(r)$ becomes zero reflects the maximum dimension of the macromolecule averaged over all orientations. The shape and the D_{max} of the $P(r)$ can be used to deduce the macromolecular shape or the distance between two domains within the protein. Both R_g and $I(0)$ can be determined from $P(r)$ as the second and zeroth moments of $P(r)$. The Q range used to compute $P(r)$ of the SecA dimer in lipid vesicles is $0.0164 < Q < 0.1$ Å^{-1} and $0.0164 < Q < 0.12$ Å^{-1} for the nucleotide-bound form of SecA. In this case, the sampling theorem is still satisfied.

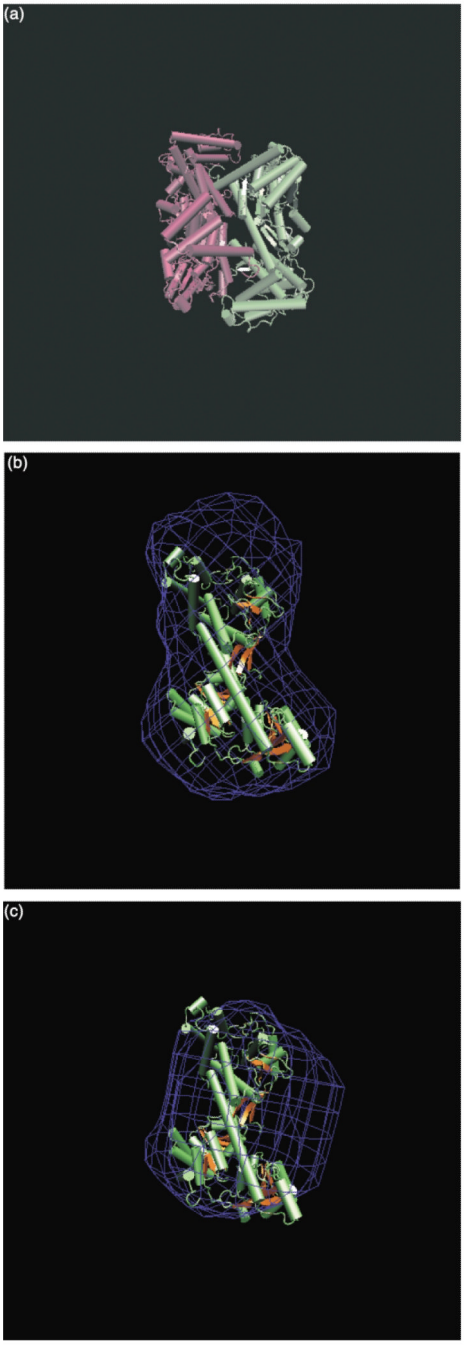

Figure 3.

Models of different forms of SecA. (a) The crystal structure of SecA dimer.[18] (b) The SANS-determined SecA–ATP-Mg^{2+} monomer structure represented by a blue wire model. This blue wire model was calculated from the SANS $P(r)$ function using the programs DAMMIN[33] and Situs.[44] The crystal structure of the apo SecA monomer was docked to the SANS model using the program Situs[44] to show that the ATP-bound monomer is more expanded than the apo SecA structure. (c) The model of SecA–ADP-Mg^{2+} calculated from SANS data (blue wire) shows that the ADP-bound monomer is more compact than the apo SecA. These images were made with VMD and are owned by the Theoretical and

Computational Biophysics Group, an NIH Resource for Macromolecular Modeling and Bioinformatics, at the Beckman Institute, University of Illinois at Urbana-Champaign.

Table 1

A summary of the size and oligomeric states of SecA measured by SANS

	$I(0)/c_{protein}$	M_w (kDa)	R_g (Å)
Apo SecA	0.033 ± 0.002	204	45.1 ± 0.9
SecA + Mg^{2+} + ATP analog	0.017 ± 0.001	105	38.3 ± 0.8
SecA + Mg^{2+} + ADP	0.019 ± 0.001	117	31.1 ± 0.5
BSA	0.011 ± 0.001	68	31.6 ± 0.2

The error in protein concentration determination is about 10%. The error in molecular mass (calibrated against BSA) is also about 10%